ELSEVIER

Nanomedicine: Nanotechnology, Biology, and Medicine
34 (2021) 102395

nanomedicine
Nanotechnology, Biology, and Medicine

nanomedjournal.com

Stabilin-1 is required for the endothelial clearance of small anionic nanoparticles

Gabriela Arias-Alpizar, MSc[a,b], Bjørn Koch, PhD[c], Naomi M. Hamelmann, MSc[d], Malene A. Neustrup, MSc[b], Jos M.J. Paulusse, PhD[d], Wim Jiskoot, PhD[b], Alexander Kros, PhD[a], Jeroen Bussmann, PhD[a,b,*]

[a]*Department of Supramolecular & Biomaterials Chemistry, Leiden Institute of Chemistry (LIC), Leiden University, RA, Leiden, The Netherlands*
[b]*Division of BioTherapeutics, Leiden Academic Centre for Drug Research (LACDR), Leiden University, RA, Leiden, The Netherlands*
[c]*Department of Molecular Cell Biology, Institute Biology Leiden (IBL), Leiden University, RA, Leiden, The Netherlands*
[d]*Department of Biomolecular Nanotechnology, MESA+ Institute for Nanotechnology and TechMed Institute for Health and Biomedical Technologies, Faculty of Science and Technology, University of Twente, AE, Enschede, The Netherlands*

Revised 25 February 2021

Abstract

Clearance of nanoparticles (NPs) after intravenous injection – mainly by the liver – is a critical barrier for the clinical translation of nanomaterials. Physicochemical properties of NPs are known to influence their distribution through cell-specific interactions; however, the molecular mechanisms responsible for liver cellular NP uptake are poorly understood. Liver sinusoidal endothelial cells and Kupffer cells are critical participants in this clearance process. Here we use a zebrafish model for liver-NP interaction to identify the endothelial scavenger receptor Stabilin-1 as a non-redundant receptor for the clearance of small anionic NPs. Furthermore, we show that physiologically, Stabilin-1 is required for the removal of bacterial lipopolysaccharide (LPS/endotoxin) from circulation and that Stabilin-1 cooperates with its homolog Stabilin-2 in the clearance of larger (~100 nm) anionic NPs. Our findings allow optimization of anionic nanomedicine biodistribution and targeting therapies that use Stabilin-1 and -2 for liver endothelium-specific delivery.

Key words: Lipopolysaccharide; Liver endothelium; Nanoparticles; Stabilin; Zebrafish

Clinical application of nanoparticles (NPs) after intravenous (*i.v.*) administration and delivery of their cargo (*i.e.* drugs, DNA, RNA, *etc*.) is hampered by the rapid sequestration of NPs, mainly by cells in the liver.[1,2] Consequently, removal of NPs with sizes above the renal filtration limit (~5.5 nm) from blood plasma[3] leads to the accumulation of most NPs in the liver. Kupffer cells (KCs), the tissue-specific macrophages that are located on the luminal side of the liver capillary vasculature (*i.e.*

Abbreviations: CCMV-VLP, cowpea chlorotic mottle virus derived virus-like particles; dpf, days post fertilization; DOPG, 1,2-dioleoyl-*sn*-glycero-3-phospho-(1'-*rac*-glycerol); ECs, endothelial cells; fluoHA, fluorescently labeled hyaluronic acid; hpi, hour(s) post injection; ISH, *in situ* hybridization; KCs, Kupffer cells; LPS, lipopolysaccharide; LSECs, liver sinusoidal endothelial cells; NP, nanoparticle; PIB-PEG, polyisobutylene-polyethylene glycol; PLGA, poly(D,L-lactide-co-glycolide); PS, polystyrene; Qdots, quantum dots; SCNPs, single chain nanoparticles; SECs, scavenging endothelial cells; siNPs, silica nanoparticles; wt, wild-type

Funding: This work was supported by the Netherlands Organization for Scientific Research (project no. 724.014.001) and by the Interreg 2 Seas Program 2014-2020 co-funded by the European Regional Development Fund under subsidy contract "Site Drug 2S07-033". The authors declare no conflict of interest. This work was presented in Nanobio&Med, Barcelona 2019.

* Corresponding author at: 2333 CC, Leiden, The Netherlands, Room GE 1.17.
E-mail addresses: g.arias.alpizar@lacdr.leidenuniv.nl, (G. Arias-Alpizar), b.e.v.koch@biology.leidenuniv.nl, (B. Koch), n.m.hamelmann@utwente.nl, (N.M. Hamelmann), m.a.neustrup@lacdr.leidenuniv.nl, (M.A. Neustrup), j.m.j.paulusse@utwente.nl, (J.M.J. Paulusse), w.jiskoot@lacdr.leidenuniv.nl, (W. Jiskoot), a.kros@chem.leidenuniv.nl, (A. Kros), j.bussmann@lacdr.leidenuniv.nl. (J. Bussmann).

https://doi.org/10.1016/j.nano.2021.102395

sinusoids), recognize and internalize NPs and were long thought to be the only liver cell type responsible for NP clearance *in vivo*. However, recent studies on the cellular distribution of NPs within the liver have revealed important contributions of B-lymphocytes, hepatocytes, hepatic stellate cells and especially liver sinusoidal endothelial cells (LSECs).[4]

The relative contribution of KCs and LSECs to the clearance of circulating NPs depends mainly on size. Phagocytosis by KCs is responsible for clearance of particles with a size >500 nm.[5,6] These NPs are captured by KCs either directly through endocytic receptors on their surface (such as scavenger and mannose receptors), or indirectly, after binding of serum proteins to the NP surface (*i.e.* opsonization) and subsequent recognition of the bound proteins by Fc- and complement receptors.[7] Compared to KCs, clearance by the more numerous LSECs (present in an approximately 1:2 ratio)[4] is largely dependent on clathrin-mediated endocytosis and is limited to particles with a size <500 nm.[8] Although for LSECs the molecular mechanisms leading to cellular NP uptake are less well understood, it is known that LSECs internalize biological colloids – such as viral particles,[9] bacterial lipopolysaccharide (LPS),[10,11] oxidized lipoprotein particles[11,12] and immune complexes[13] – at a similar rate to, or exceeding uptake by KCs.

Analysis and identification of the molecular mechanisms that mediate NP clearance will help in the challenging task of translation of nanomedicines. The analysis of LSEC function is complicated due to the rapid dedifferentiation of LSECs *in vitro*[14] and relies, consequently, on *in vivo* animal models. Recently, we have established an *in vivo* zebrafish model for NP clearance and have identified a cell type homologous to LSECs in the early zebrafish embryo.[15] These cells – which we named scavenging endothelial cells (SECs), in analogy with previously identified non-mammalian LSEC homologs[16] – are not located in the liver (as in mammals). Instead, they line the first embryonic veins and provide blood clearance before the liver vasculature becomes functional. Zebrafish is a convenient model owing to its ease of genetic manipulation and optical transparency in embryonic stages that provides the opportunity to combine genome-editing techniques and non-invasive microscopy imaging in real-time. Furthermore, zebrafish embryos are used to screen and optimize formulations prior to clinical studies. Remarkably, the clearance function of SECs and their gene expression signature in the zebrafish are comparable to those of the mammalian LSECs, as demonstrated by the presence of several endocytic receptors including several scavenger receptors.[17]

LSEC-specific scavenger receptors are prominent candidates for mediating NP clearance in this cell type, since they have been reported to interact and endocytose a wide range of ligands including modified lipoprotein particles,[12] bacterial and viral pathogens,[18] and exosomes.[19] One of the LSEC-specific scavenger receptors – Stabilin-2 – has been found to bind and internalize apoptotic bodies[20] as well as exogenous ligands, such as antisense oligonucleotides[21] and NPs.[22] Indeed, by generating a zebrafish *stab2* knockout line, we showed that Stabilin-2 is an important receptor for SEC-mediated clearance of anionic NPs.[15] However, we also observed that some negatively charged NPs were not only dependent on this receptor for clearance, demonstrated by the uptake of NPs in the SECs even in the absence of a functional Stabilin-2.

In this study, we identify a requirement for the *stab2* homolog, Stabilin-1 (encoded by *stab1* gene), in the removal of small (~6-30 nm) NPs from circulation. These two scavenger receptors have highly similar domain structure, consistent with the binding of Stabilin-1 to most (but not all) Stabilin-2 ligands *in vitro*,[23] suggestive of functional redundancy.[24] In addition, we generated *stab1/stab2* double knockout zebrafish embryos to provide evidence that Stabilin receptors complement each other in NP clearance of larger NPs (~100 nm size), as well as in the removal of bacterial LPS from the circulation. Differential scavenging function between Stabilin-1 and Stabilin-2 suggests size as a determinant for receptor specificity.

Methods

NPs

Fluorescent Alexa488-LPS from *Salmonella minnessota,* PS NPs, and Qdots layered with an organic CdSeS/ZnS and a carboxylic acid as a reactive group (consisting of a monolayer of octylamine-modified poly acrylic acid and a monolayer of poly acrylic acid -PnOAm-co-PAA- copolymer cap) were purchased from Life Technologies (Eugene, US) by Thermo Fisher Scientific and Sigma-Aldrich (The Netherlands). SiNPs were purchased from HiQ-Nano SRL (Arnesano, Italy). FluoHA was prepared through conjugation of hyaluronic acid (100 kDa) with fluorescein isothiocyanate (Isomer I, Sigma-Aldrich The Netherlands) as previously described.[25] Formulation of SCNPs and synthesis and labeling are described in this work in the Supporting Information. PLGA NPs were formulated in house with a microfluidic system. DOPG-liposomes containing 1 mol % DOPE-lissamine rhodamine were formulated with an extrusion system as described previously.[15] Rhodamine-loaded polymersomes[26] on PIB/PEG block copolymers were a kind gift from S. Askes & S. Bonnet (Leiden University, The Netherlands). Atto-647 labeled CCMV-VLPs[27] were a kind gift from R. van der Hee & J. Cornelissen (University of Twente, The Netherlands).

Zebrafish handling and strains

Zebrafish (*Danio rerio*) were maintained and handled according to the guidelines from the Zebrafish Model Organism Database (http://zfin.org) and in compliance with the directives of the local animal welfare committee of Leiden University. Housing and husbandry recommendations were followed as recommended by Alestrom et al.[28] Fertilization was performed by natural spawning at the beginning of the light period and eggs were raised at 28.5 °C in egg water (60 μg/ml Instant Ocean sea salts). The following established strains were used: *Tg(mpeg1:mCherry)*,[29] *Tg(flt1^{enh}:RFP)^{hu5333}*,[30] *Tg(flt4^{BAC}:YFP)^{hu7135}*,[31] *stab2^{ibl2}*,[15] *stab1^{ibl3}* (described in this work).

CRISPR/Cas9 mutagenesis

Cloning-free sgRNA for CRISPR/Cas9 mutagenesis was designed and synthesized as described.[32,33] 125 pg of sgRNA

(Table S2) and 300 pg cas9 mRNA were co-injected into a single-cell wt embryo fish. Primers nucleotide sequences, sgRNA sequence and predicted *stab1* and *stab2* amino acid sequences in the *stab1*^{ibl3} and *stab2*^{ibl2} were used as reported.[15] Double *stab1*^{ibl3} and *stab2*^{ibl2} mutants were generated by crossing adult homozygous zebrafish *stab2*^{ibl2} and *stab* ^{ibl3} mutants.

In situ hybridization

Whole-mount ISH was performed as described previously.[34] The sequences for probes generation (*stab1*, *stab*2, *mrc1)* were used as reported.[15]

Zebrafish i.v. microinjections and imaging

NPs formulation were injected into 2-day old zebrafish embryos (52-56 hpf) using a modified microangraphy protocol.[35] One nanoliter volume of NP formulation was calibrated and injected into the duct of Cuvier after embryos were embedded in 0.4% agarose containing 0.01% tricaine as described.[15] We created a small injection space by penetrating the skin with the injection microneedle and gently pulling the needle back, thereby creating a small pyramidal space in which the NPs were injected. Representative embryos were randomly selected according to successful injections and imaged by confocal microscopy after one hour post injection. Confocal z-stacks were captured on a Leica TCS SPE or LEICA TCS SP8 confocal microscope, using a 10× air objective (HCX PL FLUOTAR), a 40× water-immersion objective (HCX APO L), or a 63× oil-immersion objective (HC PL APO CS). In order to compare images between strains, microscopy settings (laser intensity, gain and offset) were identical between stacks and sessions. Whole-embryo images were a compilation of 3-4 overlapping z-stacks. Fiji[36] distribution of ImageJ was used to process and quantify images. At least 6 images were used for quantification.

Imaging quantification

Quantification was performed in the caudal region of the zebrafish, known to contain Stabilin endothelium and that includes the dorsal aorta, the caudal vein, and the caudal hematopoietic tissue and could include macrophages associated with SECs. First, an average intravascular intensity, within the dorsal aorta, was measured within a rectangular area in a single confocal slice that captured the center of the dorsal aorta. This measurement was repeated three times per embryo in independent sites within the dorsal aorta. Next, the maximum intensity value obtained per image was used to adjust the threshold according to the max value measure in the aorta (in circulation), generating a binary image. The strong fluorescence signal observed by accumulated phagocytosed NPs could lead to a misinterpretation of a SEC signal. For that reason and since the aim of this quantification is to compare the contribution of stabilins in the clearance of NPs and not directly the phagocytosis of macrophages, we attempt to remove the signal potentially associated with macrophages by means of size filtering (0.25-20 um) and to use a qualitative approach to refer to macrophages uptake. From the resulting image, a value of 254 was subtracted in order to get values of 0 (no signal) or 1 (fluorescence). The image of interest was multiplied (max × mask) to obtain the mean intensity and the area (%) of the analyzed image. Having these values, the total area with signal (% area × total signal /100) and the total signal (mean signal × total area) were calculated. The median intensity value of the total signal obtained from the mutants was normalized against the wt counterpart. The angle of the dorsal aspect of the dorsal aorta (a straight line) was measured and then concatenated. Images were rotated to orient the DA horizontally within the image and were subsequently cropped.

Statistical analysis

For comparisons between multiple groups, we used Kruskal–Wallis tests followed by two-tailed Dunn's tests with Bonferroni correction using the PMCMR package in R or GraphPad Prism. No statistical methods were used to predetermine sample size, but group sizes were greater than 5 in order for the null distribution of the Kruskal–Wallis statistic to approximate the X^2 distribution (with k − 1 degrees of freedom). Graphs show all individual data points and the median. Confocal image stacks (raw data) are available from the corresponding author upon request.

Results

Generation and characterization of stab1 and stab2 double knockout zebrafish

Liver endothelium is characterized by the presence of scavenger receptors strongly expressed on the membrane cell surface. Given that the clearance of some anionic NPs is not exclusively dependent on the scavenging function of Stabilin-2,[15] we hypothesized that one or more other scavenger receptor (s) expressed in LSECs might be involved in the removal of NPs. To identify additional clearance receptors, we first analyzed the RNA expression of all scavenger receptors in LSECs from mouse liver, based on published single-cell RNA sequencing datasets[37–39] (Table S1). Although this analysis revealed that *Stab2* is the most abundant scavenger receptor expressed in LSECs, the expression of seven other scavenger receptors (*Msr1, Scarb1, CD36, Scarf1, Mrc1, CXCl16* and *Stab1*) was consistently observed. Of these, the mannose receptor (*Mrc1*) and *Stab1* are the most abundant scavenger receptors expressed by LSECs besides *Stab2*. We previously reported that the zebrafish orthologues of these genes (*mrc1a* and *stab1*) are also highly expressed on SECs.[15] Since Stabilin-1 binds similar ligands as Stabilin-2,[23] we further analyzed the role of this receptor in NP clearance.

To this end, we generated a zebrafish *stab1* mutant line through CRISPR/Cas mutagenesis (guide RNA sequence in Table S2). In this strain (*stab1*^{ibl3}), a deletion of one nucleotide causes a frame-shift, leading to a premature stop codon after amino acid 85. The predicted gene product is a truncated protein lacking most conserved domains, including the fasciclin, EGF-like and LINK domains (Figure 1, *A*). This gene knockout approach allows us to study the biodistribution of NPs in zebrafish embryo and to compare the clearance by SECs in the

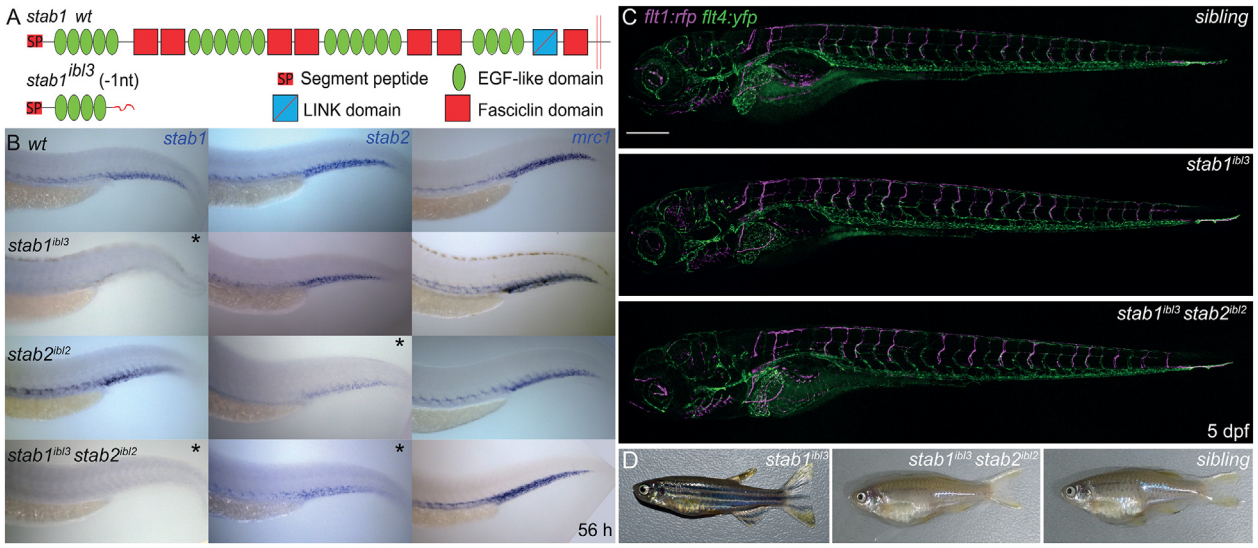

Figure 1. **Generation and characterization of *stab1* and *stab1/stab2* mutants. (A)** Schematic representation of a *stab1* domain structure predicted to be expressed from the wt Stabilin-1 and the *stab1*^{ibl3} allele. **(B)** *In situ* hybridization (ISH), mRNA expression of *stab1, stab2,* and *mrc1* in wt, *stab1*^{ibl3}, *stab2*^{ibl2} single mutants and *stab1*^{ibl3}*stab2*^{ibl2} double mutant. *Reduced expression. **(C)** Tg(*fli1:RFP fli4:YFP*) *stab1*^{ibl3} single mutant, *stab1*^{ibl3}*stab2*^{ibl2} double mutant, and sibling at 5 dpf. Scale bar: 250 μm. (d) Representative fertile adult female *stab1*^{ibl3} single mutant, *stab1*^{ibl3}*stab2*^{ibl2} double mutant and sibling zebrafish.

presence and/or absence of functional Stabilin receptor(s). To study the combined contributions of Stabilin-1 and Stabilin-2, embryos with mutations in both *stab1* and *stab2 (stab*^{DKO}*)* were also generated intercrossing *stab1*^{ibl3} and *stab2*^{ibl2} carriers.

Characterization of the generated mutants was performed by whole-mount *in situ* hybridization (ISH). Using antisense RNA probes we found a strong reduction of *stab1* expression in *stab1*^{ibl3} homozygous mutant embryos, consistent with nonsense-mediated decay (NMD) of the mutant RNA, whereas *stab2* and *mrc1a* expression was unaffected, indicating normal SEC differentiation (Figure 1, *B*). In *stab*^{DKO} embryos, expression of both *stab1* and *stab2* was also reduced through NMD. Of note, *stab2* expression was found to be slightly increased in *stab*^{DKO} compared to the signal in *stab2* mutant embryos. Importantly, *mrc1a* expression in *stab*^{DKO} embryos was maintained, indicating that SEC differentiation occurred even after the combined loss of *stab1* and *stab2*.

Homozygous *stab1* zebrafish mutants develop a normal blood and lymphatic vascular system (Figure 1, *C*) and we did not observe the previously described defects in lymphatic development induced by morpholino oligonucleotide-mediated after *stab1* knockdown.[40] *Stab1* mutant embryos develop without obvious morphological defects into viable and fertile adults (Figure 1, *D*) similar to *stab2* mutant zebrafish, as well as adult *Stab1* knockout mice. Strikingly, although *Stab1/2* double knockout mice display reduced viability due to kidney failure, adult *stab*^{DKO} zebrafish did not show increased mortality or pathology.

Identification of Stabilin-1 function in the clearance of anionic NPs

Previously, we found that two types of NPs were efficiently cleared by SECs even in the absence of *stab2* expression.[15] Specifically, these were quantum dots (Qdots) with a negatively charged surface coating and Cowpea chlorotic mottle virus derived virus-like particles (CCMV-VLPs), which are non-enveloped protein capsids with a hexagonal closed packed structure.[27] As most viruses, these VLPs have a negative surface charge. Biodistribution of the Qdots was unchanged in *stab2* mutants, while only a small reduction in the clearance of CCMV-VLPs was observed. The clearance of these two particle types, however, is apparently mediated through scavenger receptors, since it was completely inhibited by pre-injection with the general scavenger receptor inhibitor, dextran sulfate. Therefore, we injected fluorescently labeled Qdots and CCMV-VLP *i.v.* into the Duct of Cuvier of wild-type (wt), *stab1*, *stab2* and *stab*^{DKO} zebrafish embryos at 56 h post fertilization (hpf) and subsequently imaged their biodistribution with confocal microscopy. The resulting accumulation of NP fluorescence representing SEC-mediated clearance was quantified (see Methods for details) on a cellular level in the caudal region of the zebrafish tail (Figure 2, *A-B*). Importantly, this region also contains plasma-exposed macrophages, commonly known to remove NPs from circulation and analogous to the mammalian Kupffer cells (exemplified in Figure S1).

Strikingly, for both Qdots and CCMV-VLPs, we observed a strong reduction in NP clearance in both *stab1* mutants and *stab*^{DKO} embryos indicating a dominant role for Stabilin-1 in the clearance of these NP types (Figure 2, *C-F* and Figure S2, *A-B*). NPs that were cleared mainly through Stabilin-1 differ in their composition (inorganic *vs.* viral capsids) and surface chemistry, and were also chemically distinct from the NPs cleared mainly through Stabilin-2 (which included lipid and polymeric particles). The difference in surface chemistry of all NPs studied suggests a more general mechanism where particle size might be an important factor for receptor specificity. To further strengthen this hypothesis, we next injected chemically distinct (polymeric)

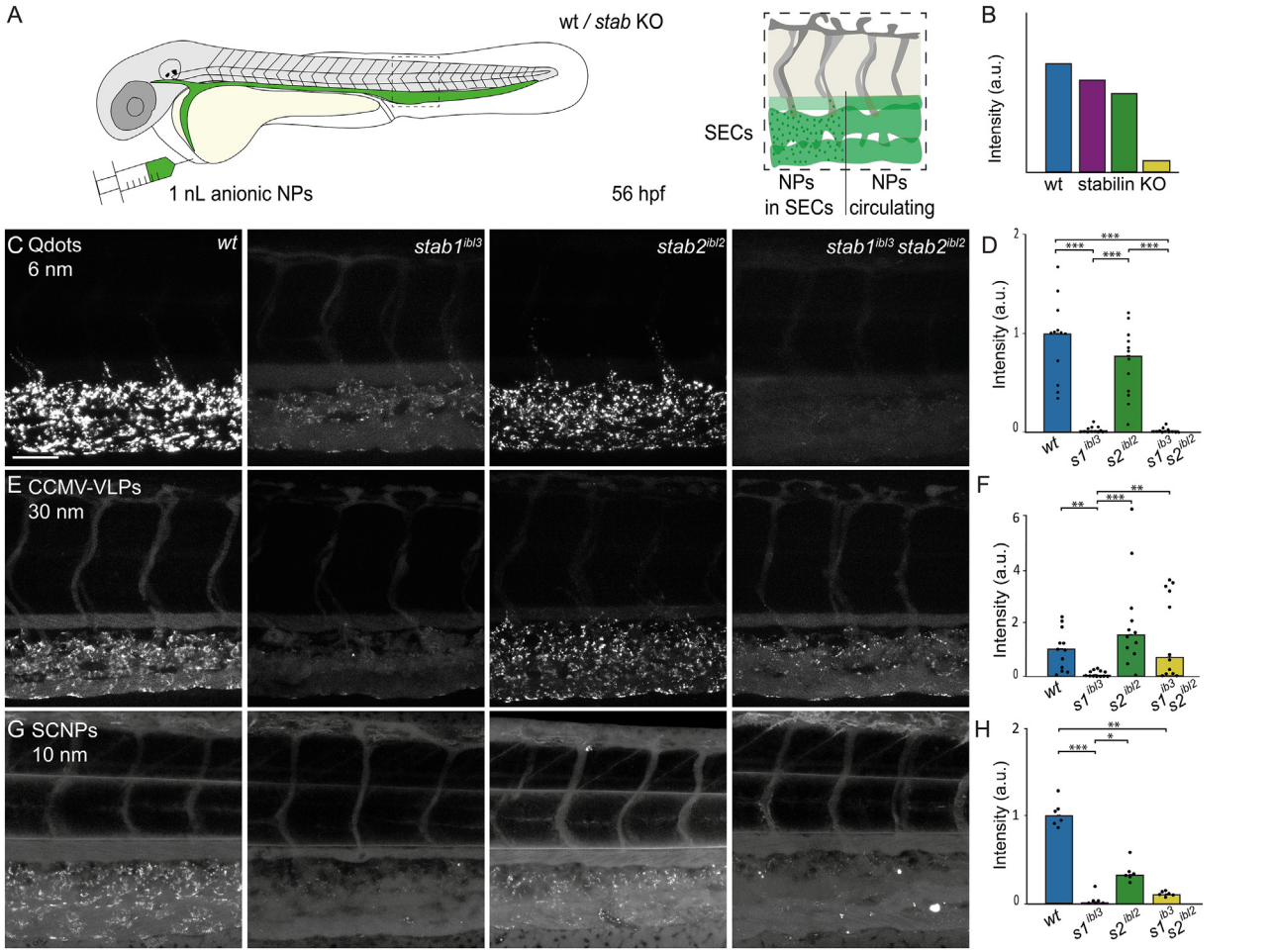

Figure 2. **Clearance of small anionic NPs occurs mainly through Stabilin-1. (A)** Schematics showing the site of injection within a 56 h post fertilization (hpf) wt or Stabilin knockout zebrafish. In a box, the caudal vein region, where SECs expressing Stabilins are located, a representation of NP circulating or cleared by SECs and **(B)** representative graph comparing intensity of fluorescent NPs in wt and stab mutants. **(C-D)** Tissue level view and quantification of fluorescently labeled Qdots. **(E-F)** CCMV-VLP **(G-H)** SCNPs. After *i.v.* injection (1 nL) in wt (AB/TL), *stab1*^{ibl3}, *stab2*^{ibl2} single mutants and *stab1*^{ibl3}*stab2*^{ibl2} double mutants at 1-1.5 hpi. Scale bar: 50 μm. Bar height represents median values, dots represent individual data points, and brackets indicate significant values (*P 0.05, **P 0.01, ***P 0.001) based on Kruskal–Wallis tests followed by two-tailed Dunn's tests with Bonferroni correction.

small NPs. To this end, fluorescently labeled anionic single-chain polymeric NPs (SCNPs) were synthesized and characterized (see Supporting Information for more details). SCNPs are a polymeric NP type which consists of biodegradable polymer chains that are covalently cross-linked and folded to form a small particle.[41] The resulting NP size is defined by the length of the polymer chain and can be used to obtain small, uniform polymer NPs of 10-20 nm. Injection of ~10 nm SCNPs in the zebrafish embryo revealed that clearance of these particles occurred through SECs as expected. Importantly, SCNP clearance was strongly affected in *stab1* mutants, similar to Qdots and CCMV-VLPs (Figure 2, *G-H* and Figure S2, *C*). These results indicate that – for negatively charged NPs – size, rather than chemical composition, is a predominant factor for receptor specificity.

Stabilin-1 and Stabilin-2 are complementary receptors in the clearance of anionic NPs by SECs

Previous studies on the biodistribution of polymer- and lipid-based NPs including polymersomes,[15,26] fibrillar supramolecular polymers,[42] solid polystyrene (PS) NPs and liposomes[15] in zebrafish *stab2* mutants revealed a residual uptake of NPs in SECs in the absence of *stab2* expression. Common characteristics of these NPs were a negative surface, but these NPs differed in size, shape, composition and rigidity.

To investigate a complementary role of Stabilin-1 to Stabilin-2 in the clearance of NPs ~100 nm, we injected negatively charged DOPG-liposomes and polymersomes in *stab*^{DKO} embryos. Interestingly, the clearance of both NPs in *stab*^{DKO} embryos was strongly affected, more than that observed in *stab2* single mutants. The loss of a functional Stabilin-1 did not affect the biodistribution of these particles compared to wt embryos (Figure 3, *A-D* and Figure S3, *A-B*), in striking contrast to the biodistribution of the smaller NPs. This indicates a cooperative role of Stabilin-1 and Stabilin-2 in NP clearance, consistent with their highly similar ligand profile.[23]

We next analyze the behavior of more rigid solid NPs. Therefore, we used anionic poly(D,L-lactide-co-glycolide) (PLGA) NPs and spherical silica NPs (siNPs) due to their

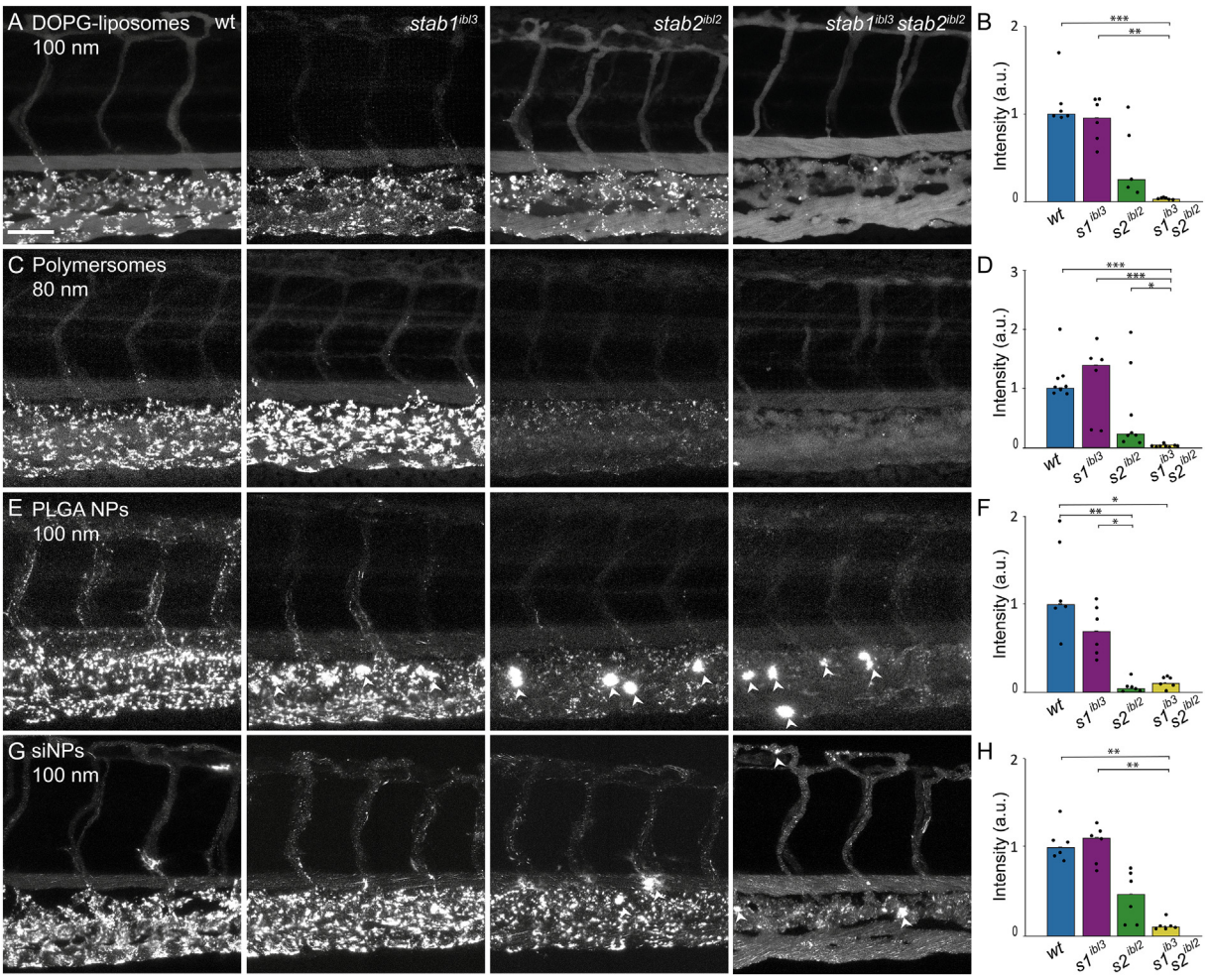

Figure 3. **Combined contribution of Stabilin-1 and Stabilin-2 in the clearance of anionic NPs. (A-B)** Tissue level view (40×) and quantification of fluorescently labeled DOPG-liposomes, **(C-D)** polymersomes, **(E-F)** PLGA NPs, **(G-H)** siNPs after *i.v.* injection (1 nL) in wt (AB/TL), *stab1*^{ibl3}, *stab2*^{ibl2} single and *stab1*^{ibl3}*stab2*^{ibl2} double mutants at 1-1.5 h post injection (hpi). White arrows indicate apparent NP uptake within plasma-exposed macrophages. Scale bar: 50 μm. Graphs represent intensity of fluorescent NPs in wt and *stab* mutants. Bar height represents median values, dots are individual data points, and brackets indicate significant values (*P 0.05, **P 0.01, ***P 0.001) based on Kruskal–Wallis tests followed by two-tailed Dunn's tests with Bonferroni correction.

relevant importance in drug delivery or biomedical imaging agent applications.[43,44] Similar to polymersomes and DOPG-liposomes, anionic PLGA NPs and siNPs are cleared through SECs in wt zebrafish. Their biodistribution remained unchanged in stab1 mutants, but clearance was strongly affected in stab2 mutants, and even more in stab^{DKO} mutants (Figure 3, *E-H* and Figure S3, *C-D*). Interestingly, for the PLGA NPs, the absence of SEC clearance resulted in increased macrophage uptake (indicated by white arrows in Figure 3, *E, G* and Figure S1). The absence of molecular interactions between NPs for most of the ~100 nm NPs and SECs in the stab^{DKO} embryos is an evidence of a combined contribution of Stabilin-1 and Stabilin-2, where Stabilin-2 is the predominant receptor involved in the clearance in this size range. However, this contribution seems to be a more complex process that depends not only on size but also on the particle composition. We observed the behavior for anionic NP type (polystyrene NPs) of different sizes (40-100 nm) (Figure S4, *A*). In this case, we first qualitatively confirmed SEC-uptake of these particles through co-injection with fluorescently labeled hyaluronic acid (fluoHA), a Stabilin-2 ligand and a marker for SEC endocytosis (Figure S4, *B-C*). SEC clearance is only partly affected in stab^{DKO} mutants, indicating the presence of at least one additional clearance receptor besides Stabilin-1 and Stabilin-2 (Figure S4, *D-G*).

Identification of an endogenous Stabilin ligand: bacterial LPS

Clearance of synthetic nanoparticles can only be reflective of physiological mechanisms that are required for the removal of naturally occurring particles in the 10 to 200 nm size range. We therefore sought to identify naturally occurring circulating particles of this dimension as a probable physiologic Stabilin ligand. One such ligand is LPS, which is the main component of the outer membrane of Gram-negative bacteria with the lipid A portion, an anchor in the bacterial cell wall, which provides toxicity and activates immune responses in mammals.[45]

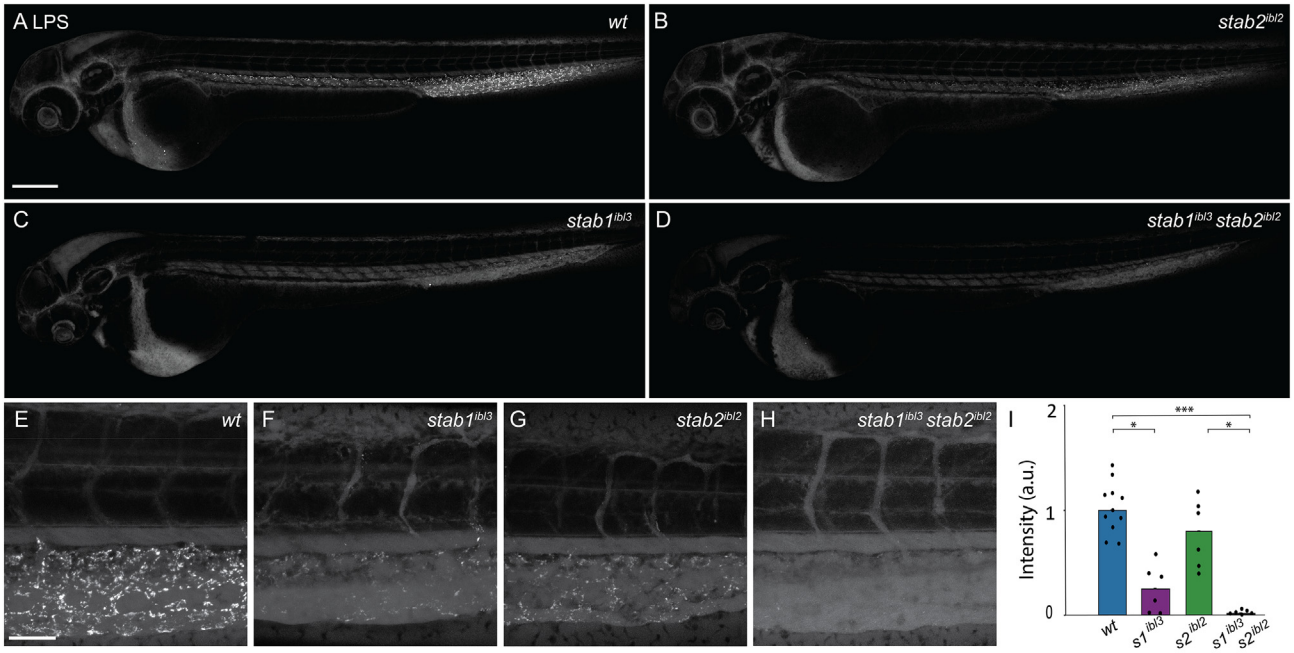

Figure 4. **LPS clearance is mediated by Stabilin-1 and Stabilin-2. (A)** Biodistribution of Alexa488 LPS (1 nL of 500 μm/mL) in wt (AB/TL), **(B)** *stab2*^{ibl2} mutant, **(C)** *stab1*^{ibl3} mutant, **(D)** *stab1*^{ibl3}*stab2*^{ibl2} double mutant at 56 hpf, 1.5 hpi, whole body view (10×). Scale bar: 200 μm. **(E-H)** Tissue level views, caudal region (40×). Scale bar: 50 μm **(I)** Graph represents intensity of fluorescent LPS in wt and stab mutants. Bar height represents median values, dots represent individual data points, and brackets indicate significant values (*P 0.05, ***P 0.001) based on Kruskal–Wallis tests followed by two-tailed Dunn's tests with Bonferroni correction. The images shown in **E-H** correspond to the fish used in **A-D** and are one of the images used for the graph in **I**.

We rationally hypothesized that bacterial endotoxin LPS would be one of this natural ligands for three reasons. First, LPS is highly toxic and must be rapidly eliminated from host circulation, which is performed mainly by LSECs scavenger receptors of unknown identity.[10,18] Second, due to its amphiphilic nature, LPS self-assembles into small anionic NPs with a diameter of ~50 nm, resembling synthetic NPs.[46,47] Third, Stabilin-2 has been shown to bind to Gram-negative bacteria – which contain LPS – *in vitro*.[48] To investigate whether circulating LPS is indeed cleared by SECs through Stabilin receptors, fluorescently labeled LPS (Alexa488-LPS) from the Gram-negative bacterium *Salmonella minnesota*[49] was *i.v.* administered. LPS diluted into a salt suspension is proposed to aggregate into micelles at concentrations above the critical micelle concentration (CMC).[46,47,50] The LPS concentration injected (500 μg/ml) is above the CMC (~10 μg/ml)[50] even after dilution into the blood of a zebrafish embryo (estimated 30-fold dilution factor, excluding red blood cells, at 2 dpf).[51] Distribution of fluorescent LPS in *Tg*(*mpeg1:mCherry*) zebrafish shows no extensive co-localization with labeled macrophages (Figure S5). This result indicates that phagocytosis by plasma-exposed macrophages does not represent the main clearance route of LPS in the zebrafish embryo, at 56 hpf. Instead, LPS was associated mainly with SECs located in the caudal vein region of wt zebrafish (Figure 4, *A, E*), confirming their functional homology to mammalian LSECs.[10]

Next, we injected LPS in stab2, stab1 and double mutant zebrafish embryos (Figure 4, *B-D, F-H*). Association of LPS with SECs was maintained in stab2 mutants (Figure 4, *B, G*). In this case, although a slight decrease in the LPS clearance was observed compared to wt embryos, SEC-uptake was not significantly changed between these two groups (Figure 4, *I*). Importantly, LPS uptake by SECs was reduced in stab1 knockout and completely abrogated in stab^{DKO} mutants, leading to a strong increased level of LPS in circulation (Figure 4, *D, H*). This result revealed a cooperative function of Stabilin-1 and Stabilin-2 in LPS uptake and clearance. The loss of LPS uptake in the double knockouts was very similar to that observed after pre-administration of a competitive inhibitor dextran sulfate (Figure S6), indicating LPS is a common ligand for Stabilin-1 and Stabilin-2, and both receptors are redundantly required for the removal of LPS from the circulation.

Discussion

The understanding of NPs *in vivo* behavior of their molecular and cellular interactions after *i.v.* administrations is essential to improve efficacy and pharmacokinetics of nanomaterials. Here, we identify that Stabilin-1, a scavenger receptor expressed in LSECs in mammals, is involved in the clearance of small anionic NPs. Interestingly, while mice lacking both *Stab1* and *Stab2* revealed a glomerulofibrotic nephropathy secondary to impaired liver clearance of noxious blood factors[52,53] leading to strongly reduced viability, we observed that *stab*^{DKO} adult zebrafish were obtained in mendelian ratios and were phenotypically indistinguishable from single mutant and wt zebrafish. Since the reduced viability observed in *Stab1/Stab2* double knockout mice is due

mainly to kidney failure, the viability of *stab*^{DKO} fish potentially reflects the high regenerative capacity of the zebrafish kidney.[54]

Through comparison of NP biodistribution in wt and single/ double Stabilin mutants we could quantify the relative contribution of Stabilin receptors to the clearance of specific NPs in zebrafish embryos. The analysis of physicochemical properties (Table S3) and *in vivo* biodistribution of NPs involved in differential uptake, for both Stabilin receptors, revealed a dependency on size of the particle. Particle size is a critical parameter affecting cellular uptake of nanotherapeutics.[55] Depending on the intended application – *i.e.* drug targeting, vaccine delivery or nucleic acid delivery – an optimal size range is desired.[56,57] In addition, improved internalization associated with small nanoparticles (~25-50 nm) has been previously shown.[58,59] Gold nanoparticles of this size range coated with antibodies, for example, display improved endocytosis and regulation of cellular functions.[58] Similarly, ~25-50 nm range has been suggested as an optimal size to reach the maximum cellular uptake.[59] For *in vivo* activity of small particles, NP clearance by the liver is an important factor influencing biodistribution, but so far has not been linked to a specific receptor. The preference between Stabilin-1 and Stabilin-2 could be attributed indirectly to biological factors or to differences in the structural domains. Biologically, although NP protein corona formation *in vivo* is known to affect the fate of NPs, the different chemistries of the various NPs involved in this study strongly suggest that charge and size are predominant requirements in the interactions between NPs and Stabilin receptors. Structurally, both receptors are initially expressed as a 310 kDa protein, have a very similar domain structure, and are known to share a very common ligand binding profile.[23] So far, it is unknown which structural differences could explain the differential requirement for both receptors to NP clearance.

Besides NPs, the identification of an endogenous ligand of Stabilins, LPS, provides important information in the mechanism of clearance of endotoxins. Mechanistically, LPS is known to be detected through toll-like receptor factor 4 and myeloid differentiation factor 2 (TLR4/Md-2) complex in mammals.[60] Inflammatory responses to LPS have been previously observed in the zebrafish,[5] but the signaling involved in LPS-sensing is not well understood. Since SECs in the zebrafish are functionally homologous to LSECs[15] and LPS is known to be recognized by LSECs in mammals,[10,18] we believe our results contribute to the mechanistic understanding of recognition and clearance of endotoxin LPS – especially at high concentrations above the CMC – important not only in the identification and study of host–pathogen interactions but also in inflammation and immunity responses.

In conclusion, by using the zebrafish as model that allows genetic analysis and imaging of NP clearance *in vivo*, we demonstrate that Stabilin-1 is required independently of Stabilin-2 for endothelial clearance of small anionic Qdots, CCMV-VLP, and SCNPs (6-30 nm) from the circulation. Since NPs with very different chemistries are cleared by Stabilin-1, this strongly suggests negative surface charge and size as the predominant factors that determine a requirement for Stabilin-1 in NP clearance. We also show a combined contribution between Stabilin-1 and Stabilin-2 in the clearance of anionic liposomes, polymeric PS and siNPs (~100 nm) and in the removal of LPS. These results reveal a partial redundancy between *stab1* and *stab2*, both important for NPs clearance, and suggest a differential uptake where size is one of the key parameters determining the selective uptake by each receptor. Given size is particularly important in vaccine development, biomedical imaging applications and delivery technologies, improved mechanistic insights into the interactions between size-selected NPs and the liver at the molecular level contribute to the optimization of small nanomaterials and avenues for receptor-specific targeting.

Associated Content

Supporting Information: Tables, figures, methods, characterization of all NPs used and synthesis and formulation of SCNPs.

Author Information

Credit Author Statement

G.A-A.: Conceptualization, methodology, validation, formal analysis, investigation, writing original draft preparation, project administration. **B.K.:** Investigation, writing - reviewing & editing. **N.H., M.N.,** and **J.P.:** Resources, investigation. **W.J.** and **A.K.:** Project administration, funding acquisition, writing reviewing & editing. **J.B.:** Conceptualization, methodology, validation, formal analysis, investigation, writing review & editing, supervision, project administration. The manuscript was written through contributions of all authors. All authors have given approval to the final version of the manuscript. The authors declare no competing financial interest.

Acknowledgments

We thank F. Campbell for a critical reading of the manuscript and providing DOPG-liposomes. S. Askes/ S. Bonnet (Leiden University, the Netherlands) and J. Cornelissen/ R. van der Hee (University of Twente) are acknowledged for providing polymersomes and CCMV-VLP respectively. We also thank the Institute of Biology Leiden (Leiden University, The Netherlands) and caretakers of zebrafish facility. This work was supported by the Netherlands Organization for Scientific Research (project no. 724.014.001) and by the Interreg 2 Seas Program 2014-2020 co-funded by the European Regional Development Fund under subsidy contract "Site Drug 2S07-033".

Appendix A. Supplementary data

Associated Content

Supporting Information: Tables, figures, methods, characterization of all NPs used and synthesis and formulation of SCNPs. Supplementary data to this article can be found online at https://doi.org/10.1016/j.nano.2021.102395.

References

1. Zhang YN, Poon W, Tavares AJ, McGilvray ID, Chan WCW. Nanoparticle-liver interactions: cellular uptake and hepatobiliary elimination. *J Control Release* 2016;**240**:332-48, https://doi.org/10.1016/j.jconrel.2016.01.020.

2. Polo E, Collado M, Pelaz B, Del Pino P. Advances toward more efficient targeted delivery of nanoparticles in vivo: understanding interactions between nanoparticles and cells. *ACS Nano* 2017;**11**(3):2397-402, https://doi.org/10.1021/acsnano.7b01197.
3. Choi HS, Liu W, Misra P, Tanaka E, Zimmer JP, Itty Ipe B, et al. Renal clearance of quantum dots. *Nat Biotechnol* 2007;**25**(10):1165-70, https://doi.org/10.1038/nbt1340.
4. Tsoi KM, MacParland SA, Ma XZ, Spetzler VN, Echeverri J, Ouyang B, et al. Mechanism of hard-nanomaterial clearance by the liver. *Nat Mater* 2016;**15**(11):1212-21, https://doi.org/10.1038/nmat4718.
5. Hayashi Y, Takamiya M, Jensen PB, Ojea-Jimenez I, Claude H, Antony C, et al. Differential nanoparticle sequestration by macrophages and scavenger endothelial cells visualized in vivo in real-time and at ultrastructural resolution. *ACS Nano* 2020;**14**(2):1665-81, https://doi.org/10.1021/acsnano.9b07233.
6. Shiratori Y, Tananka M, Kawase T, Shiina S, Komatsu Y, Omata M. Quantification of sinusoidal cell function in vivo. *Semin Liver Dis* 1993;**13**(1):39-49, https://doi.org/10.1055/s-2007-1007336.
7. Tenzer S, Docter D, Kuharev J, Musyanovych A, Fetz V, Hecht R, et al. Rapid formation of plasma protein corona critically affects nanoparticle pathophysiology. *Nat Nanotechnol* 2013;**8**(10):772-81, https://doi.org/10.1038/nnano.2013.181.
8. Rejman J, Oberle V, Zuhorn IS, Hoekstra D. Size-dependent internalization of particles via the pathways of clathrin- and caveolae-mediated endocytosis. *Biochem J* 2004;**377**(Pt 1):159-69, https://doi.org/10.1042/BJ20031253.
9. Breiner KM, Schaller H, Knolle PA. Endothelial cell-mediated uptake of a hepatitis B virus: a new concept of liver targeting of hepatotropic microorganisms. *Hepatology* 2001;**34**(4 Pt 1):803-8, https://doi.org/10.1053/jhep.2001.27810.
10. Yao Z, Mates JM, Cheplowitz AM, Hammer LP, Maiseyeu A, Phillips GS, et al. Blood-borne lipopolysaccharide is rapidly eliminated by liver sinusoidal endothelial cells via high-density lipoprotein. *J Immunol* 2016;**197**(6):2390-9, https://doi.org/10.4049/jimmunol.1600702.
11. van Oosten M, van de Bilt E, van Berkel TJ, Kuiper J. New scavenger receptor-like receptors for the binding of lipopolysaccharide to liver endothelial and Kupffer cells. *Infect Immun* 1998;**66**(11):5107-12.
12. Li R, Oteiza A, Sorensen KK, McCourt P, Olsen R, Smedsrod B, et al. Role of liver sinusoidal endothelial cells and stabilins in elimination of oxidized low-density lipoproteins. *Am J Physiol Gastrointest Liver Physiol* 2011;**300**(1):G71-81, https://doi.org/10.1152/ajpgi.00215.2010.
13. Wohlleber D, Knolle PA. The role of liver sinusoidal cells in local hepatic immune surveillance. *Clin Transl Immunology* 2016;**5**(12)e117, https://doi.org/10.1038/cti.2016.74.
14. Sellaro TL, Ravindra AK, Stolz DB, Badylak SF. Maintenance of hepatic sinusoidal endothelial cell phenotype in vitro using organ-specific extracellular matrix scaffolds. *Tissue Eng* 2007;**13**(9):2301-10, https://doi.org/10.1089/ten.2006.0437.
15. Campbell F, Bos FL, Sieber S, Arias-Alpizar G, Koch BE, Huwyler J, et al. Directing nanoparticle biodistribution through evasion and exploitation of Stab2-dependent nanoparticle uptake. *ACS Nano* 2018;**12**(3):2138-50, https://doi.org/10.1021/acsnano.7b06995.
16. Seternes T, Sorensen K, Smedsrod B. Scavenger endothelial cells of vertebrates: a nonperipheral leukocyte system for high-capacity elimination of waste macromolecules. *Proc Natl Acad Sci U S A* 2002;**99**(11):7594-7, https://doi.org/10.1073/pnas.102173299.
17. Wong KS, Proulx K, Rost MS, Sumanas S. Identification of vasculature-specific genes by microarray analysis of Etsrp/Etv2 overexpressing zebrafish embryos. *Dev Dyn* 2009;**238**(7):1836-50, https://doi.org/10.1002/dvdy.21990.
18. Hampton RY, Golenbock DT, Penman M, Krieger M, Raetz CR. Recognition and plasma clearance of endotoxin by scavenger receptors. *Nature* 1991;**352**(6333):342-4, https://doi.org/10.1038/352342a0.
19. Verweij FJ, Revenu C, Arras G, Dingli F, Loew D, Pegtel DM, et al. Live tracking of inter-organ communication by endogenous exosomes in vivo. *Dev Cell* 2019;**48**(4):573-89 e574https://doi.org/10.1016/j.devcel.2019.01.004.
20. Park SY, Jung MY, Kim HJ, Lee SJ, Kim SY, Lee BH, et al. Rapid cell corpse clearance by stabilin-2, a membrane phosphatidylserine receptor. *Cell Death Differ* 2008;**15**(1):192-201, https://doi.org/10.1038/sj.cdd.4402242.
21. Miller CM, Donner AJ, Blank EE, Egger AW, Kellar BM, Ostergaard ME, et al. Stabilin-1 and Stabilin-2 are specific receptors for the cellular internalization of phosphorothioate-modified antisense oligonucleotides (ASOs) in the liver. *Nucleic Acids Res* 2016;**44**(6):2782-94, https://doi.org/10.1093/nar/gkw112.
22. Alidori S, Bowman RL, Yarilin D, Romin Y, Barlas A, Mulvey JJ, et al. Deconvoluting hepatic processing of carbon nanotubes. *Nat Commun* 2016;**7**:12343, https://doi.org/10.1038/ncomms12343.
23. Harris EN, Cabral F. Ligand binding and signaling of HARE/Stabilin-2. *Biomolecules* 2019;**9**(7):273, https://doi.org/10.3390/biom9070273.
24. Nowak MA, Boerlijst MC, Cooke J, Smith JM. Evolution of genetic redundancy. *Nature* 1997;**388**(6638):167-71, https://doi.org/10.1038/40618.
25. de Belder AN, Wik KO. Preparation and properties of fluorescein-labelled hyaluronate. *Carbohydr Res* 1975;**44**(2):251-7, https://doi.org/10.1016/s0008-6215(00)84168-3.
26. Askes SH, Pomp W, Hopkins SL, Kros A, Wu S, Schmidt T, et al. Imaging upconverting polymersomes in cancer cells: biocompatible antioxidants brighten triplet-triplet annihilation upconversion. *Small* 2016;**12**(40):5579-90, https://doi.org/10.1002/smll.201601708.
27. Verwegen M, Cornelissen JJ. Clustered nanocarriers: the effect of size on the clustering of CCMV virus-like particles with soft macromolecules. *Macromol Biosci* 2015;**15**(1):98-110, https://doi.org/10.1002/mabi.201400326.
28. Alestrom P, D'Angelo L, Midtlyng PJ, Schorderet DF, Schulte-Merker S, Sohm F, et al. Zebrafish: housing and husbandry recommendations. *Lab Anim* 2019, https://doi.org/10.1177/0023677219869037 23677219869037.
29. Ellett F, Pase L, Hayman JW, Andrianopoulos A, Lieschke GJ. mpeg1 promoter transgenes direct macrophage-lineage expression in zebrafish. *Blood* 2011;**117**(4):e49-56, https://doi.org/10.1182/blood-2010-10-314120.
30. Bussmann J, Bos FL, Urasaki A, Kawakami K, Duckers HJ, Schulte-Merker S. Arteries provide essential guidance cues for lymphatic endothelial cells in the zebrafish trunk. *Development* 2010;**137**(16):2653-7, https://doi.org/10.1242/dev.048207.
31. Hogan BM, Herpers R, Witte M, Helotera H, Alitalo K, Duckers HJ, et al. Vegfc/Flt4 signalling is suppressed by Dll4 in developing zebrafish intersegmental arteries. *Development* 2009;**136**(23):4001-9, https://doi.org/10.1242/dev.039990.
32. Varshney GK, Pei W, LaFave MC, Idol J, Xu L, Gallardo V, et al. High-throughput gene targeting and phenotyping in zebrafish using CRISPR/Cas9. *Genome Res* 2015;**25**(7):1030-42, https://doi.org/10.1101/gr.186379.114.
33. Carrington B, Varshney GK, Burgess SM, Sood R. CRISPR-STAT: an easy and reliable PCR-based method to evaluate target-specific sgRNA activity. *Nucleic Acids Res* 2015;**43**(22)e157, https://doi.org/10.1093/nar/gkv802.
34. Thisse C, Thisse B. High-resolution in situ hybridization to whole-mount zebrafish embryos. *Nat Protoc* 2008;**3**(1):59-69, https://doi.org/10.1038/nprot.2007.514.
35. Weinstein BM, Stemple DL, Driever W, Fishman MC. Gridlock, a localized heritable vascular patterning defect in the zebrafish. *Nat Med* 1995;**1**(11):1143-7.
36. Schindelin J, Arganda-Carreras I, Frise E, Kaynig V, Longair M, Pietzsch T, et al. Fiji: an open-source platform for biological-image analysis. *Nat Methods* 2012;**9**(7):676-82, https://doi.org/10.1038/nmeth.2019.
37. Halpern KB, Shenhav R, Massalha H, Toth B, Egozi A, Massasa EE, et al. Paired-cell sequencing enables spatial gene expression mapping of liver

endothelial cells. *Nat Biotechnol* 2018;**36**(10):962-70, https://doi.org/10.1038/nbt.4231.
38. Sabbagh MF, Heng JS, Luo C, Castanon RG, Nery JR, Rattner A, et al. Transcriptional and epigenomic landscapes of CNS and non-CNS vascular endothelial cells. *Elife* 2018;**7**, https://doi.org/10.7554/eLife.36187.
39. Schaum N, Karkanias J, Neff NF, May AP, Quake SR, Wyss-Coray T, et al. Single-cell transcriptomics of 20 mouse organs creates a Tabula Muris. *Nature* 2018;**562**(7727):367-72, https://doi.org/10.1038/s41586-018-0590-4.
40. Stoll SJ, Bartsch S, Kroll J. HOXC9 regulates formation of parachordal lymphangioplasts and the thoracic duct in zebrafish via stabilin 2. *PLoS One* 2013;**8**(3)e58311, https://doi.org/10.1371/journal.pone.0058311.
41. Kroger APP, Hamelmann NM, Juan A, Lindhoud S, Paulusse JMJ. Biocompatible single-chain polymer nanoparticles for drug delivery—a dual approach. *ACS Appl Mater Interfaces* 2018;**10**(37):30946-51, https://doi.org/10.1021/acsami.8b07450.
42. Saez Talens V, Arias-Alpizar G, Makurat DMM, Davis J, Bussmann J, Kros A, et al. Stab2-mediated clearance of supramolecular polymer nanoparticles in zebrafish embryos. *Biomacromolecules* 2020;**21**(3):1060-8, https://doi.org/10.1021/acs.biomac.9b01318.
43. Davis ME, Chen ZG, Shin DM. Nanoparticle therapeutics: an emerging treatment modality for cancer. *Nat Rev Drug Discov* 2008;**7**(9):771-82, https://doi.org/10.1038/nrd2614.
44. Rezvantalab S, Drude NI, Moraveji MK, Güvener N, Koons EK, Shi Y, et al. PLGA-based nanoparticles in cancer treatment. *Frontiers in Pharmacology* 2018;**9**(1260), https://doi.org/10.3389/fphar.2018.01260.
45. Raetz CR, Whitfield C. Lipopolysaccharide endotoxins. *Annu Rev Biochem* 2002;**71**:635-700, https://doi.org/10.1146/annurev.biochem.71.110601.135414.
46. Sasaki H, White SH. Aggregation behavior of an ultra-pure lipopolysaccharide that stimulates TLR-4 receptors. *Biophys J* 2008;**95**(2):986-93, https://doi.org/10.1529/biophysj.108.129197.
47. Wang C, Nelson T, Chen D, Ellis JC, Abbott NL. Understanding lipopolysaccharide aggregation and its influence on activation of factor C. *J Colloid Interface Sci* 2019;**552**:540-53, https://doi.org/10.1016/j.jcis.2019.05.013.
48. Adachi H, Tsujimoto M. FEEL-1, a novel scavenger receptor with in vitro bacteria-binding and angiogenesis-modulating activities. *J Biol Chem* 2002;**277**(37):34264-70, https://doi.org/10.1074/jbc.M204277200.
49. Triantafilou K, Triantafilou M, Fernandez N. Lipopolysaccharide (LPS) labeled with Alexa 488 hydrazide as a novel probe for LPS binding studies. *Cytometry* 2000;**41**(4):316-20.
50. Aurell CA, Wistrom AO. Critical aggregation concentrations of gram-negative bacterial lipopolysaccharides (LPS). *Biochem Biophys Res Commun* 1998;**253**(1):119-23, https://doi.org/10.1006/bbrc.1998.9773.
51. Craig MP, Gilday SD, Dabiri D, Hove JR. An optimized method for delivering flow tracer particles to intravital fluid environments in the developing zebrafish. *Zebrafish* 2012;**9**(3):108-19, https://doi.org/10.1089/zeb.2012.0740.
52. Palani S, Elima K, Ekholm E, Jalkanen S, Salmi M. Monocyte Stabilin-1 suppresses the activation of Th1 lymphocytes. *J Immunol* 2016;**196**(1):115-23, https://doi.org/10.4049/jimmunol.1500257.
53. Schledzewski K, Geraud C, Arnold B, Wang S, Grone HJ, Kempf T, et al. Deficiency of liver sinusoidal scavenger receptors stabilin-1 and -2 in mice causes glomerulofibrotic nephropathy via impaired hepatic clearance of noxious blood factors. *J Clin Invest* 2011;**121**(2):703-14, https://doi.org/10.1172/JCI44740.
54. Diep CQ, Ma D, Deo RC, Holm TM, Naylor RW, Arora N, et al. Identification of adult nephron progenitors capable of kidney regeneration in zebrafish. *Nature* 2011;**470**(7332):95-100, https://doi.org/10.1038/nature09669.
55. Hoshyar N, Gray S, Han H, Bao G. The effect of nanoparticle size on in vivo pharmacokinetics and cellular interaction. *Nanomedicine (Lond)* 2016;**11**(6):673-92, https://doi.org/10.2217/nnm.16.5.
56. Hassett KJ, Benenato KE, Jacquinet E, Lee A, Woods A, Yuzhakov O, et al. Optimization of lipid nanoparticles for intramuscular administration of mRNA vaccines. *Mol Ther Nucleic Acids* 2019;**15**:1-11, https://doi.org/10.1016/j.omtn.2019.01.013.
57. Sykes EA, Chen J, Zheng G, Chan WC. Investigating the impact of nanoparticle size on active and passive tumor targeting efficiency. *ACS Nano* 2014;**8**(6):5696-706, https://doi.org/10.1021/nn500299p.
58. Jiang W, Kim BY, Rutka JT, Chan WC. Nanoparticle-mediated cellular response is size-dependent. *Nat Nanotechnol* 2008;**3**(3):145-50, https://doi.org/10.1038/nnano.2008.30.
59. Zhang S, Li J, Lykotrafitis G, Bao G, Suresh S. *Size-dependent endocytosis of nanoparticles Adv Mater* 2009;**21**:419-24, https://doi.org/10.1002/adma.200801393.
60. Nagai Y, Akashi S, Nagafuku M, Ogata M, Iwakura Y, Akira S, et al. Essential role of MD-2 in LPS responsiveness and TLR4 distribution. *Nat Immunol* 2002;**3**(7):667-72, https://doi.org/10.1038/ni809.